**UNIVERSITY POLITEHNICA of BUCHAREST**
Faculty of Mechanical Engineering and Mechatronics
Thermodynamics, Heat engines, Thermal and Refrigerating Equipment

# PH.D. THESIS

## Increasing the efficiency of energy systems through cogeneration and the use of waste or renewable sources

**Author:** Eng. Mihaela Ciocan

**Scientific advisor:** Ph.D. Professor Alexandru Șerban

**Content**

## 1. THE CURRENT STATE OF RESEARCH IN THE FIELD

Under the pressure of climate change, society has only two options:

1. To slow down the rate of industrial development with the repercussion of the decrease in the supply of jobs with the consequence of the reduction in the standard of living, or
2. To continue economic development more effectively with the reduction of polluting effects aiming at a society with zero greenhouse gas emissions.

In order for the climate balance to be balanced, all the ways of absorbing the existing greenhouse gases from the atmosphere must be found and applied, and for industrial and consumer production to be oriented towards zero emissions in order to stabilize the global temperature.

Today's society is characterized by a continuous increase in the need for energy, determined on the one hand by the continuous economic development of practically all regions, but primarily by the "new industrial countries" such as China and India, and on the other hand by world population growth (Aboelwafa et al., 2018).

Society must maintain the global warming target of 1.5 K above the situation existing in the pre-industrial era (1850 – 1900), a limit allowed due to policies to reduce poverty and improve the standard of living of the population.

To achieve this, precise targets have been set, such as the "CO2 budget" which determines the amount that a person, or country, is allowed to emit. For example in Germany, which is one of the top seven CO2 polluters, each inhabitant emits around 10 t CO2 per year, while only 1 t CO2 would be acceptable (https://www.ipcc.ch/sr15/).

Zero net emissions means reducing as close as possible to zero the emissions that would accompany energy production technologies, and what would remain to be absorbed from the atmosphere by algae in ocean water, by land that can accumulate carbon from plant residues, by trees forests in their growth have in wood products, or captures of CO2 extracted from the air by chemical processes and stored in the ground (https://www.un.org/en/climatechange/net-zero-coalition)

The earth's atmosphere is currently 1.1 K warmer on average than it was in the late 1800s. To keep the warming target to no more than 1.5 K, as stipulated in the 2015 Paris Agreement, greenhouse emissions must reduced by 55% by 2030 compared to 1990, and reach zero in 2050 (https://climate.ec.europa.eu/eu-action/european-green-deal/european-climate-law_en).

The energy sector is responsible for 75% of current greenhouse gas emissions, and to reduce and eventually eliminate them, the replacement of the coal and fossil fuel-based power generation system in general with solar and wind systems is expected.
(https://climate.ec.europa.eu/eu-action/european-green-deal/european-climate-law_en).

-


Fig.1.1 Directions of the European Green Deal
(https://commission.europa.eu/strategy-and-policy/priorities-2019-2024/european-green-deal_en).

Most of the carbon emissions are due to the conventional process of producing electricity by burning fossil fuels.

The problem of ensuring the growing energy needs is all the more important as energy production by classical methods is also associated with the increase in greenhouse gas emissions and global warming.

The inclusion of natural gas and nuclear energy in the category of transitional green energies allows a respite until the total technological and economic maturity is reached for the production of green electricity with zero carbon emissions (https://www.cnbc.com/2022/07/06/europe-natural-gas-nuclear-are-green-energy-in-some-circumstances-.html).
The devastating effect of releases into the atmosphere for some substances of industrial interest can be traced based on the Global Warming Potential (GWP).

## 2. METHODS OF THERMODYNAMIC ANALYSIS APPLIED IN THE OPTIMIZATION STUDY OF THE CYCLES OF POWER, COOLING AND HEAT GENERATING SYSTEMS

The study of the behavior of a thermodynamic system is based on the realization of its mathematical model with the help of which the operation and construction of the system can be simulated (Moran et al., 2011,Feidt, 2006,Borel and Favrat, 2010).

The mathematical model is composed of the analytical expressions of the general laws of nature, which each component process of the system and the system as a whole must respect. In addition to obeying the laws of nature, the mathematical model also contains information about the economic constraints and thermodynamic properties of the system. The mathematical model must take into account the interaction of the considered system with the physical and economic environment in which it evolves. The thermodynamic and economic analysis method used imposes the mathematical model.

For the thermal sciences, the main general laws of nature are formulated by the First and Second Principles.

Based on these two principles, phenomenological thermodynamics has built methods for analyzing thermal systems.

The thermodynamic analysis methods are the following:

2.1 The energetic method, based on the First Principle of Thermodynamics and the notion of energy, in which the quality of the energy or its meaning does not matter, only the quantity. An analysis based exclusively on the first Principle of thermodynamics takes into account neither the physical environment nor the economic environment in which the system in question evolves.

2.2 The entropic method, based on the Second Principle of thermodynamics, introduces the state quantity: entropy.
The entropic approach highlights the meaning of unfolding processes in nature and reveals that real processes are irreversible - they have a preferential evolution.

2.3 The exergetic method that introduces the notion of exergy. Exergy is the measure of the imbalance of a system in relation to its environment (Moran et al., 2011, Bejan et al., 1996).

- The environment means the part of the external environment with which the system interacts. It is considered that the ambient environment is large enough so that its intensive thermal, mechanical and chemical parameters( $T_0, p_0, \mu_k^0$ ) remain constant after interaction with the considered system.
- Exergy represents the measure of the imbalance of a system in relation to its surrounding environment (Moran et al., 2011,Bejan et al., 1996).

It is considered a system that is out of balance with its surrounding environment.

The imbalance can be thermal( $T \neq T_0$ ), mechanic ( $p \neq p_0$ ) or chemical ( $\mu_{k0} \neq \mu_k^0$ ).

The state of equilibrium with the surrounding environment is generically called the dead state. Nothing usable can be obtained from a system that is dead.

If the system is only in mechanical disequilibrium with respect to the environment ( $p \neq p_0$, $T = T_0, \mu_{k0} = \mu_k^0$ ) there are two possibilities:

a. $p \rangle p_0$ - the system in its evolution towards mechanical equilibrium with its surrounding environment produces mechanical work. If the processes are reversible, the mechanical work produced is maximum;

b. $p \langle p_0$ - to bring the system into a state of equilibrium with the environment, mechanical work must be consumed. If all processes are reversible, the mechanical work consumed is minimal.

.

### 2.3.3. Thermomechanical exergy of a control volume

The thermomechanical exergy of a control volume represents the maximum amount of mechanical work that a flowing system can release.

For 1 kg of agent in the flow, the exergy becomes:

$$ex_{ec} = h - h_0 - T_0(s - s_0) + \frac{w^2}{2} + gz \qquad (2.6)$$

where $h(T, p)$ and $s(T, p)$ correspond to the system that is at T and p, and $h_0(T_0, p_0)$ and $s_0(T_0, p_0)$ are the state quantities corresponding to the system when the latter is in thermomechanical equilibrium with the environment.

### 2.3.4. Exergy of heat

The exergy of a quantity of heat Q characterized by a temperature T when the temperature of the environment is $T_0$, It is:

$$Ex_Q^T = Q\left(1 - \frac{T_0}{T}\right) \qquad (2.7)$$

a. When $T \rangle T_0$, the heat exergy represents the maximum mechanical work that can be produced by a Carnot cycle that evolves between the temperature T of the heat and the temperature T0 of the environment;

b When $T < T_0$, the heat exergy represents the minimum mechanical work that must be consumed by a reversed Carnot cycle to transport the heat Q from the temperature level T to the level T0.

### 2.3.5. Chemical exergy

When the system has a composition different from that of its surroundings, it is possible to produce work by letting the system change from its original composition to the composition of its surroundings. At the end of the process, the elements of the considered system diffuse among the corresponding elements of the environment. In the release process, the system only interacts with the environment. There are two situations:

a. System consisting of elements that are in its ambient environment, but in a different composition. Example; a kmol of gaseous mixture of40% $O_2$ and 60%$N_2$ in molar participation is in thermomechanical equilibrium with the ambient environment ($T = T_0$ , $p = p_0$). The ambient environment is represented by dry air with the molar composition $x^0_{O_2} = 0{,}21$ and $x^0_{N_2} = 0{,}79$

A kmol of oxygen to reach the level of oxygen molecules in its surrounding medium can expand isothermally reversibly releasing the maximum mechanical work:

$$\bar{e}x_{O_2} = \bar{R} \quad T_0 \quad \ln \frac{x_{O_2}}{x^0_{O_2}} \tag{2.8}$$

One kmol of nitrogen to reach the partial pressure of nitrogen in the ambient medium must be compressed. The minimum mechanical work consumed corresponds to a reversible isothermal compression:

$$\bar{e}x_{N_2} = \bar{R} \cdot T_0 \cdot \ln \frac{x_{N_2}}{x^0_{N_2}} \tag{2.9}$$

For one kmol of mixture, the chemical exergy is:

$$\bar{e}x^{CH} = x_{O_2} \cdot \bar{R} \cdot T_0 \cdot \ln \frac{x_{O_2}}{x^0_{O_2}} + x_{N_2} \cdot \bar{R} \cdot T_0 \cdot \ln \frac{x_{N_2}}{x^0_{N_2}} \tag{2.10}$$

In general:

$$\bar{e}x^{CH} = \bar{R} \cdot T_0 \cdot \sum x_i \ln \frac{x_i}{x^0_i} \tag{2.11}$$

b. The exergy of a system that interacts with existing elements in the environment releasing work and transforming into elements that diffuse among the elements of the environment. Example: A fuel whose general formula is $C_aH_b$ and a gaseous medium in which water is in vapor state

$$\bar{e}x^{CH}_{C_aH_b} = \bar{g}^0_{f,C_aH_b} - a \cdot \bar{g}^0_{f,CO_2} - \frac{b}{2} \cdot \bar{g}_{f,H_2O(g)} + \bar{R} \cdot T_0 \cdot \ln \frac{\left(x^0_{O_2}\right)^{\left(a+\frac{b}{4}\right)}}{\left(x^0_{CO_2}\right)^a \cdot \left(x^0_{H_2O}\right)^{\frac{b}{2}}} \tag{2.12}$$

where $\bar{g}_{f,i}^{0}$ is the Gibbs function of formation at $T = T_0$ and $p = p_0$ of component i in the compound.

### 2.3.6. Exergetic balance equation for a control volume

Considering only the exergy of each form of energy, a balance equation can be written in which all forms of energy regardless of their category (ordered or disordered) are brought to a common level.

Using the energy balance (First principle) and entropy (Second principle) equations, the exergetic balance equation for a system represented by a control volume (Fig. 2.4) in steady state becomes:

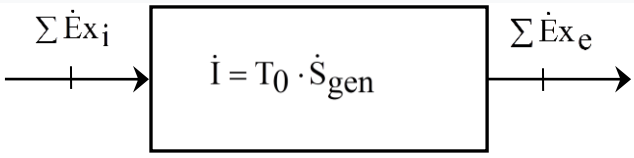


Fig. 2.4 Exergy balance scheme for a control volume

$$\sum \dot{E}x_i = \sum \dot{E}x_e + T_0 \cdot \dot{S}_{gen} \tag{2.13}$$

Noting that for real (irreversible) processes $\dot{S}_{gen} \geq 0$, we get:

$$\dot{I} = T_0 \cdot \dot{S}_{gen} \geq 0 \tag{2.14}$$

quantity that represents the amount of exergy consumed during the irreversible process.

It follows that exergy is a quantity that cannot be conserved.

$$\sum \dot{E}x_i \geq \sum \dot{E}x_e \tag{2.15}$$

Equality is for ideal, reversible processes

Highlighting the exergetic product and the exergetic fuel of the system, equation (2.13) becomes:

$$\dot{E}x_{Cb} = \dot{E}x_P + \sum \dot{E}x_{Pi} + \sum \dot{I} \tag{2.16}$$

The exergetic yield of the system becomes:

$$\eta_{ex} = \frac{\dot{E}x_P}{\dot{E}x_{Cb}} = 1 - \frac{\sum \dot{E}x_{Pi} + \sum \dot{I}}{\dot{E}x_{Cb}} \tag{2.17}$$

The exergetic analysis method takes into account not only the amount of a certain form of energy, but also the intensive parameters of the environment with which the system interacts. The exergetic analysis method does not take into account the economic environment.

## 2.4. The exergoeconomic method.

The only method that takes into account the quantity and quality of a certain form of energy, taking into account the interactions of the system with the physical environment and the economic environment in which it evolves, is the exergoeconomic analysis (Bejan et al., 1996,El-Sayed, 2003). To account for the economic environment in which a thermal system operates, each internal exergy destruction must be assigned a cost.

Exergoeconomic analysis succeeds in assigning a cost (exergic or monetary) to each destruction of usable energy as a result of an irreversible process occurring within the system (Dobrovicescu and Tsatsaronis, 2006), (Lozano and Valero, 1993), (Thick, 2000).

## 3. COMPARATIVE ANALYSIS OF INDIVIDUAL AND COGENERATION SYSTEMS OF MECHANICAL POWER AND HEAT WITH STEAM TURBINE PLANTS

## 3.1 Introduction

Energy consumption for urban or industrial heating and electricity are in most cases concurrent.

Domestic, industrial or social energy consumption manifests itself simultaneously through the need for thermal and electrical energy.

Thermal energy or heat can be produced individually with separate installations, but the most efficient way is through cogeneration.

Important research focuses on improving the efficiency and construction of cogeneration systems.

The chapter analyzes from the point of view of the First and Second Principles of Thermodynamics the advantages of producing heat and mechanical power, each individually or by cogeneration.

## 3.2 Energy or exergetic analysis – a comparative study of individual heat and electricity production systems

For the separate production of electricity and heat, a steam turbine plant and a separate hot water boiler are considered.

The schematic of the steam turbine system and the boiler are shown in figures (3.1) and (3.2). The two systems are used for energy recovery of household waste.

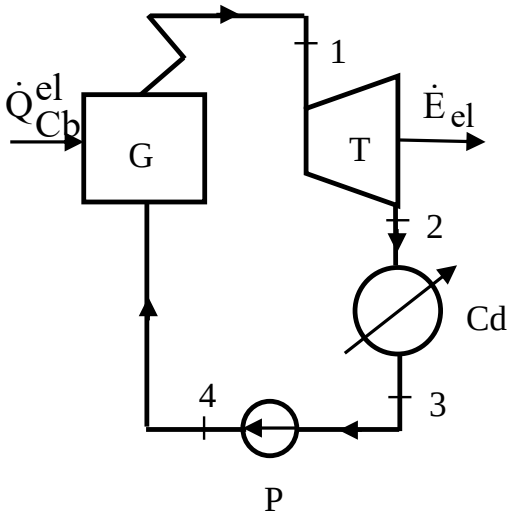


Figure 3.1 Scheme of the steam turbine plant

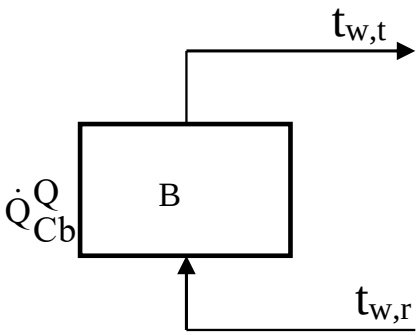


Figure 3.2 Functional diagram of the hot water boiler

## 3.3. Production of heat and electricity by cogeneration in a back pressure steam turbine system

The scheme of the cogeneration plant of heat and electric energy with a back pressure steam turbine plant is shown in figure 3.16

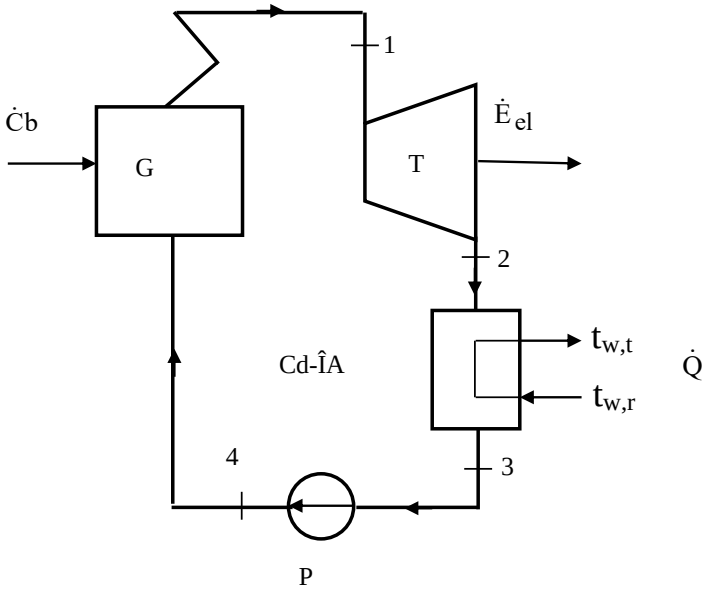


Figure 3.16. Combined heat and power system with co-pressure steam turbine plant

### 3.4 Conclusions

The energy analysis indicates only the energy losses transferred to the external environment. It cannot make any qualitative difference between different types of energies.

For the hot water boiler only the loss of 10% ($\varphi_{L\,WB}$ =0.1 or $\eta_{wB}$= 0.9) due to incomplete insulation leads to an energy performance COPen=0.9 and not unitary.

On the other hand, from an energetic point of view, the conversion of thermal energy into mechanical work (electrical energy) seems to be less efficient. For the low energy yield of the steam turbine installation $COP_{en}^{el}$ =0.27, the energy analysis finds the capacitor as the culprit whose loss is 63% of the installation's energy consumption.

# 4. EXERGETIC ANALYSIS OF COLD AND HOT COGENERATION SYSTEMS

## 4.1. Introduction

The study deals with a cogeneration system for the food industry with the role of heat pump and refrigeration plant characterized by two products - cooling and heating (Şerban et al., 2018).

The working agent is ammonia, an ecological refrigerant harmless to the environment. The paper develops a technique for searching for optimal regimes from a functional and constructive point of view, using the exergetic analysis method (Dobrovicescu A., 2000).

## 4.2 Scheme of the refrigeration plant

It is considered a refrigeration system that provides two products – heating and cooling. To quantify the useful effect of each of the two products, the analysis is based on the concept of exergy (Kousskou et al., 2006).

Figure 4.1 shows the functional scheme and the representation of the duty cycle in the ph diagram of the considered system. Working agent R717 (NH3).

## 4.3 Exergetic analysis

The exergetic analysis was carried out at the level of the consumer, which on both the cold and hot side is represented by water as a carrier of cold and heat.

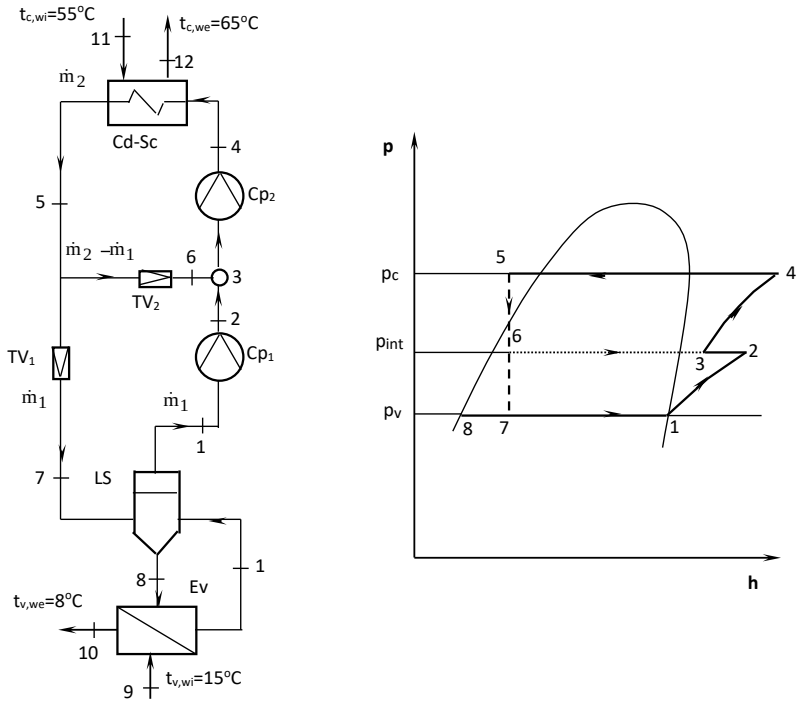


(a) (b)

Figure 4.1 Refrigeration and heat pump installation.
(a) Functional scheme of the installation; (b) Representation of the duty cycle in the ph diagram

The products offered to the consumer are represented by the exergies of the heat extracted from the vaporizer $\left|\dot{E}x_{Qv}^{T_{v,w}}\right|$ at the level of water temperature as a cold carrier and condenser respectively $\left|\dot{E}x_{Qc}^{T_{c,w}}\right|$ at the level of water temperature as a heat carrier.

In order to quantify the destruction and exergy losses associated with the production of the two products, the vaporizer and the condenser will be studied separately.

## 4.4. Performance coefficients of the cogeneration system

To highlight the overall Product and Fuel of the cogeneration system and trace the factors causing the inefficiency, the exergetic balance equation is written:

$$\left|\dot{L}_{cp1,t}\right| + \left|\dot{L}_{cp2,t}\right| + \left|\dot{L}_{P1,t}\right| + \left|\dot{L}_{P2,t}\right| = \left(\dot{E}x_{10}^{T} - \dot{E}x_{9}^{T}\right) + \left(\dot{E}x_{12}^{T} - \dot{E}x_{11}^{T}\right) + \dot{I}_{cp1} + \\ + \dot{P}i_{cp1,m,el} + \dot{I}_{cp2} + \dot{P}i_{cp2,m,el} + \dot{I}_{c,f} + \dot{I}_{c,\Delta T} + \dot{P}i_{c,P} + \dot{I}_{t1} + \\ + \dot{I}_{t2} + \dot{I}_{v,\Delta T} + \dot{L}_{v,f} + \dot{L}_{v,P} \qquad (4.16)$$

Based on the energy and exergetic balances, the energy and exergetic performance coefficients become:

$$\eta_t = \frac{\left|\dot{Q}_{01}\right| + \left|\dot{Q}_{c1}\right|}{\sum \dot{W}_t} \qquad (4.17)$$

$$\eta_{ex} = \frac{\Delta\dot{E}x_v^T + \Delta\dot{E}x_c^T}{\sum \dot{W}_t} \qquad (4.18)$$

For the condenser, respectively the evaporator, the local exergetic yields are:

$$\eta_{ex,ev} = \frac{\dot{P}_v}{\dot{F}_v} \qquad (4.19)$$

$$\eta_{ex,cd(gh)} = \frac{\dot{P}_{cd}}{\dot{F}_{cd}} \qquad (4.20)$$

### 4.5 The influence of the variation of the decisional parameters

The temperature levels at which cold and heat are supplied to the consumer are specified by the project (Figure 4.1).

The optimal value of the intermediate pressure is obtained following a parametric study of the evolution of the performance coefficients (Figures 4.4).

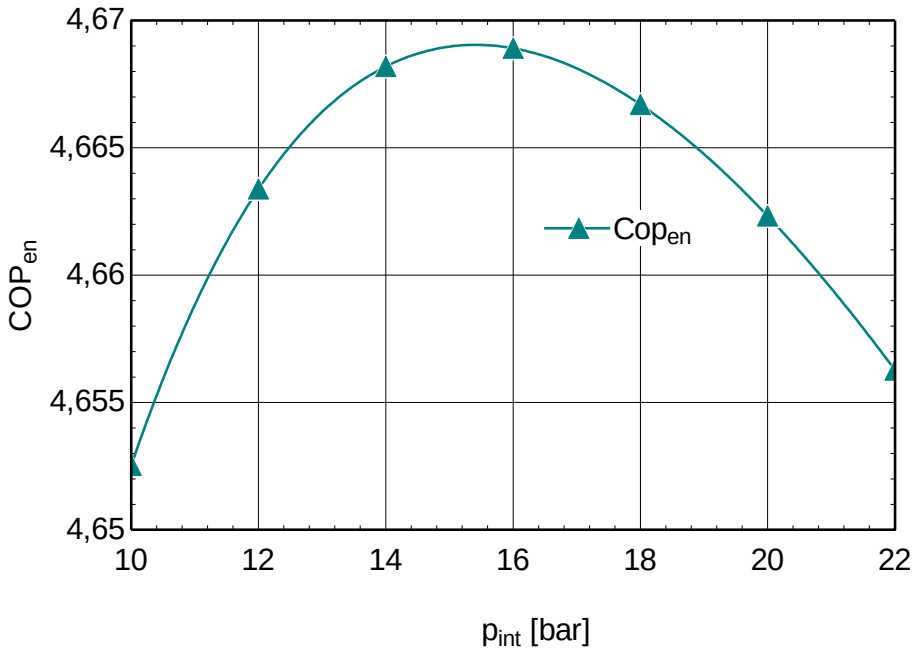


Figure 4.4 The global coefficient of energy performance depending on the intermediate pressure

It is observed that for an intermediate compression pressure of $p_2$ = 1.5 MPa both the energy and exergetic performance coefficients reach maximum values. $COP_{en}$ $\eta_{ex}$

**4.6 Conclusions**

The exergetic balance of the system indicates for each of the devices the "product" and the "fuel".

Exergy losses and destruction are highlighted for each dissipative zone.

For the vaporizer, the exergy of the heat generated in the friction process must be removed by the refrigeration system, thus increasing the power consumption of the compressor.

For the condenser, the heat energy generated by friction represents an exergy destruction caused by the irreversibility of friction.

# 5. ANALYSIS OF THE ENERGY POTENTIAL OF MUNICIPAL WASTE USED AS FUEL

## 5.1 Introduction

The energy recovery of municipal waste is a priority for cities with a sustainable economy with a double impact on the environment - it helps to reduce landfills and lead to a reduction in conventional fossil fuel consumption.

## 5.2 Chemical analysis of a fuel obtained from municipal solid waste

The elemental analysis was carried out using a COSTECH ECS 4010 type analyzer which works on the principle of chromatographic analysis. Combustion products were identified on a quantitative basis.

To determine the elemental analysis, several samples of 1.5-4 mg were taken from each type of municipal waste analyzed.

For four samples of municipal waste, elemental analysis was performed (chemical composition in percent by mass).

To determine the waste and moisture content of the samples presented above, a technical analysis is performed. The amounts of ash and moisture were determined with a Nabertherm furnace (Fig. 5.1) and a Polenko Model SLM 53ECO furnace (Fig. 5.2), respectively.


Figure 5.1. Nabertherm furnace for determining ash content

Figure 5.2. Poleko oven - Model SLW 53 ECO for the determination of moisture content

The elemental analysis for four municipal waste samples, where the symbols represent percentages of mass composition and the lower calorific value (LHV) value of each sample are shown in Table 1.
Sulfur is absent from each municipal waste sample.
It follows that municipal waste has a significant calorific value that can be utilized by direct combustion or by co-combustion with a support fuel.
The samples were selected from the landfills located in the areas with the largest population and the most heterogeneous generation (from the population, street, restaurants, markets).

## 5.3 Chemical exergy of fuel obtained from municipal solid waste

In order to highlight the maximum production capacity of useful energy (mechanical or electrical energy) through energy recovery of municipal solid waste, the chemical exergy of each sample of municipal waste was calculated.

For each municipal waste sample, the dry and ashless fuel composition was given (Table 2).

Table 5.2 Composition of dry and ashless household solid waste

| **DSM** | **Mass composition [** $\frac{\text{kg constituent}}{\text{kg combustibil}}100$ **]** | | | | | **Molar composition [** $\frac{\text{kmol / nr.atoms}}{\text{kg combustibil}}$ **]** | | | | |
|---|---|---|---|---|---|---|---|---|---|---|
| | **c** | **H** | **N** | **S** | **A** | **c** | **h** | **n** | **S** | **a** |
| Sample 1 | 54.73 | 6,828 | 3,356 | - | 35.09 | 0.0456 | 0.0683 | 0.0024 | - | 0.0219 |
| Sample 2 | 46.75 | 5,664 | 1,464 | - | 46.12 | 0.0390 | 0.0566 | 0.0010 | - | 0.0288 |
| Sample 3 | 71.78 | 7,988 | 5,035 | - | 15.2 | 0.0598 | 0.0799 | 0.0036 | - | 0.0095 |
| Sample 4 | 73.4 | 8,278 | 5,351 | - | 12.97 | 0.0611 | 0.0828 | 0.0038 | - | 0.0081 |

The chemical combustion reaction is given by the stoichiometric equation:

$$(cC + hH + oO + nN) + \nu_{O_2} O_2 \rightarrow \nu_{CO_2} CO_2 + \nu_{H_2O} H_2O(l) + \nu_{N_2} N_2 \qquad (5.1)$$

where c, h, o, n are given by Table 5.3 and C, H, O, N are the combustible elements.

The model used for the calculation of chemical exergy is based on a system composed of the combustion chamber and a part of the environment with which the fuel interacts (Figure 5.3)

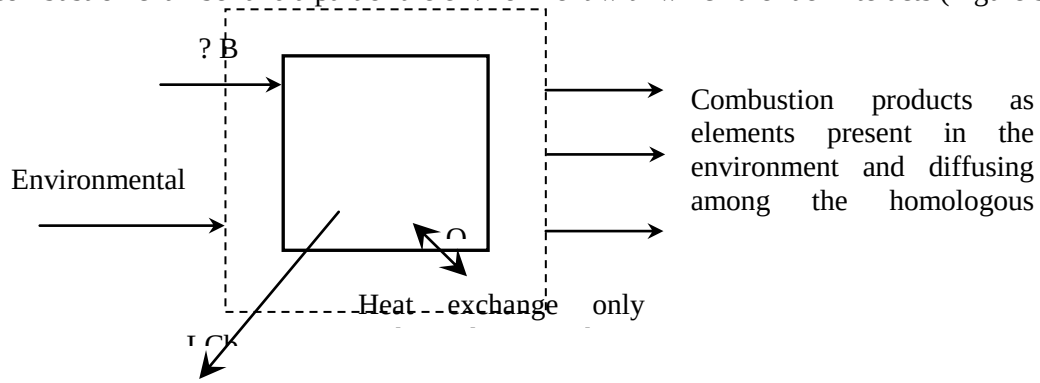


Figure 5.3 Schematic of the composite system consisting of the fuel, the reaction chamber and the ambient environment

The reactants enter and the products leave the combustion chamber at ambient parameters (P0, T0). Oxygen is taken from the ambient environment where it is found at its partial pressure $p_{O2}^0$ the products of combustion diffuse into the ambient medium among the homologous components of the ambient medium which are found in the ambient medium at their partial pressure $p_i^0$.

Following the schematic model based on the Van't Hoff balance chamber (Fig. 5.4), the chemical exergy for 1 kg of dry and ash-free fuel becomes:

$$\bar{ex}_{Cb}^{ch} = L_{max,Cch} + \gamma_{CO_2} \bar{ex}_{CO_2}^{ch} + \gamma_{H_2O} \bar{ex}_{H_2O}^{ch}(l) + \gamma_{N_2} \bar{ex}_{N_2}^{ch} - \gamma_{O_2} \bar{ex}_{O_2}^{ch} \qquad (5.2)$$

in which $L_{\max,CCh}$ is the maximum thing the combustion chamber can release and $\bar{ex}_i^{ch}$ are the chemical exergies of the reactants and products, with the exception of the fuel, entering and leaving the combustion chamber respectively, being in thermal and mechanical equilibrium with the ambient environment.

The energy balance combined with the entropy balance of the combustion chamber, under the conditions in which the chemical reaction takes place reversibly, without, therefore, generating entropy, gives:

$$L_{max,CCh} = -\Delta G_0 = -[(\nu_{CO_2}\bar{h}_{CO_2,0} + \nu_{H_2O}\bar{h}_{H_2O(l),0} + \nu_2\bar{h}_{N_2,0} - h_{F,0} - \nu_{O_2}\bar{h}_{O_2,0}) -$$
$$- T_0\,(\nu_{CO_2}\bar{s}_{CO_2,0} + \nu_{H_2O}\bar{s}_{H_2O(l),0} + \nu_2\bar{s}_{N_2,0} - s_{F,0} - \nu_{O_2}\bar{s}_{O_2,0})] =$$
$$= (h_{Cb,0} + \nu_{O_2}\bar{h}_{O_2,0} - \nu_{CO_2}\bar{h}_{CO_2,0} - \nu_{H_2O}\bar{h}_{H_2O(l),0} - \nu_{N_2}\bar{h}_{N_2,0}) -$$
$$- T_0(s_{Cb,0} + \nu_{O_2}\bar{s}_{O_2,0} - -\nu_{CO_2}\bar{s}_{CO_2,0} - \nu_{H_2O}\bar{s}_{H_2O(l)} - \nu_{N_2}\bar{s}_{N_2,0}) \quad (5.3)$$

in which $\bar{h}_{i,0}$ is the molar enthalpy of formation of component i in thermomechanical equilibrium with its ambient environment and, $\bar{s}_{i,0}$ is the absolute molar entropy at T0 and P0.

The first bracket in the right-hand side of equation (5.3) represents the higher calorific value (HHV) of the fuel considered.

$$HHV = (h_{Cb,0} + \nu_{O_2}\bar{h}_{O_2,0} - \nu_{CO_2}\bar{h}_{CO_2,0} - \nu_{H_2O}\bar{h}_{H_2O(l),0} - \nu_{N_2}\bar{h}_{N_2,0}) \quad (5.4)$$

Taking into account this observation, the relation (5.3) becomes:

$$L_{max,CCh} = HHV - T_0(s_{Cb,0} + \nu_{O_2}\bar{s}_{O_2,0} - \nu_{CO_2}\bar{s}_{CO_2,0} - \nu_{H_2O}\bar{s}_{H_2O(l)} - \nu_{N_2}\bar{s}_{N_2,0}) \quad (5.5)$$

The value of the higher calorific value of a dry and ashless fuel can be estimated as follows (W. Eiserman et al. 1980):

$$HHV = [152{,}19H/100 + 98{,}767][C/100/3 + H/100 - (O/100 - S/100)/8 \ \frac{MJ}{kg} \quad (5.6)$$

The absolute entropy of a dry, ashless fuel can be estimated with the relation (W. Eiserman, et al., 1980)

$$s_{Cb,0} = c[37{,}1653 - 31{,}4767\exp(-0{,}564682\frac{h}{c+n}) + 20{,}1145\frac{o}{c+n} + 54{,}3111\frac{n}{c+n} +$$
$$+ 44{,}6712\frac{s}{c+n}]\ \frac{kJ}{kgK} \quad (5.7)$$

The values for H, C, O and h, c, n, o are shown in Table 5.2.

To calculate the chemical exergies of combustion gases and oxygen as components of the medium, the following standard molar composition of the medium is considered:

$$\bar{x}^0_{N_2} = 0.7567\,;\ \bar{x}^0_{O_2} = 0.2035\,;\ \bar{x}^0_{H_2O(g)} = 0.0312\,;\ \bar{x}^0_{CO_2} = 0.0003$$

The superscript 0 indicates that the component is at its ambient partial pressure.

The chemical exergy of each element or component that does not react with elements of the environment but can be found as a constituent of the environment is given by the mechanical work of compression/expansion at the temperature of the environment from the pressure of the environment to the partial pressure at which the homologous component is found in the environment.

The superscript 0 indicates that the component is at ambient partial pressure.

$$e\bar{x}^{ch}_i = \bar{R}T_0 \ln\frac{p_0}{\bar{x}^0_i p_0} = \bar{R}T_0\frac{1}{\bar{x}^0_i} \quad (5.8)$$

## 5.4 Conclusions

The paper presents an experimental methodology for estimating the chemical composition of municipal solid waste. Even though the composition of DSM resulting mainly from food residues is not homogeneous. The chemical exergy of each sample recommends the use of DSM as a single fuel or in co-combustion with another fuel.

The chemical exergy calculation model of DSM is very useful for exergetic and exergoeconomic analysis of power plants using DSM as fuel. The exergetic and exergoeconomic analysis allow finding out the true efficiency of an energy system and give direction to operational and constructive optimization.

# 6. THERMAL SOLAR COLLECTORS

## 6.1. Introduction

### 6.1.1. General considerations

Today's society is characterized by a continuous increase in the need for energy, determined on the one hand by the continuous economic development of practically all regions, but primarily by the "new industrial countries" such as China and India, and on the other hand by world population growth (Aboelwafa et al, 2018).

The problem of ensuring the growing energy needs is all the more important as energy production by classical methods is also associated with the increase in greenhouse gas emissions and global warming.

Solar energy and the Rankine cycle can also be used in cogeneration or trigeneration systems.

- Heat can be obtained directly from solar radiation or can be extracted from the water-steam Rankine cycle.
- Electricity can be obtained through Rankine cycles with water - steam or with organic substances.
- Cold can be obtained from heat with the help of absorption or adsorption installations.

The following presents the possibilities of converting solar energy into heat and then into electricity using the Rankine cycle, respectively into cold using the absorption cycle.

### 6.1.2. Systems for converting solar energy into electricity through the Rankine cycle

The accompanying figures show some schematics of plants that operate after the Steam Rankine Cycle (SRC) and use solar radiation as an energy source.

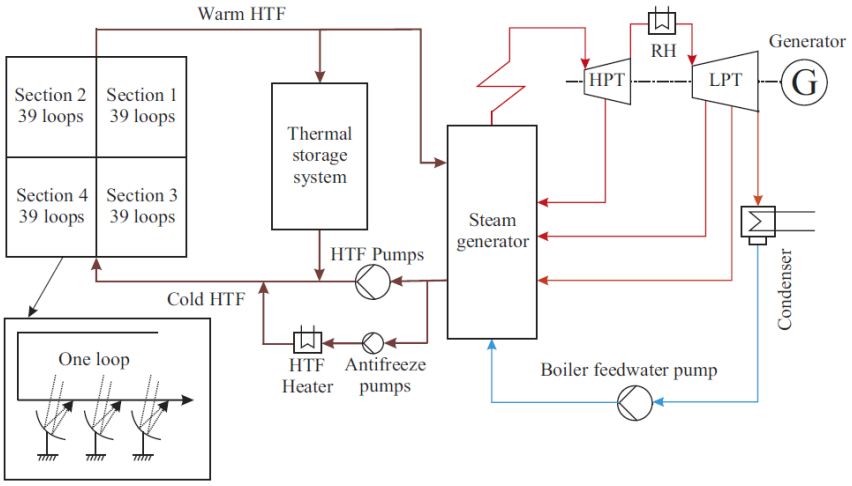


Solar SRC installation (Andasol II - Spain) (Al-Maliki et al., 2016)

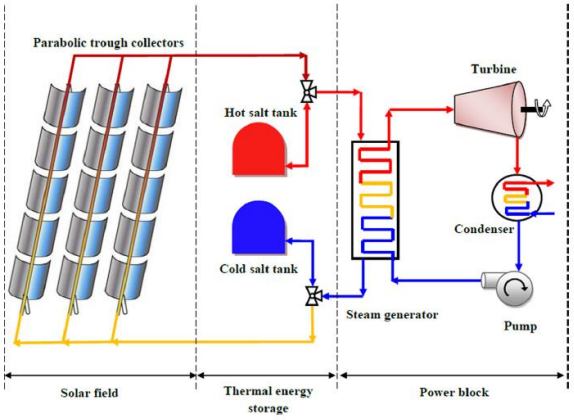


Solar SRC installation
with parabolic concentrators
(Belgasim et al., 2018)

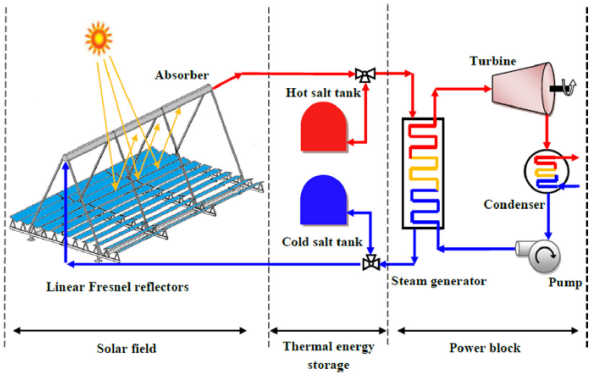


Solar SRC installation
with linear concentrators
(Belgasim et al., 2018)

In the accompanying figures, some schematics of installations are shown that work according to the Rankine cycle with organic agents (Organic Rankine Cycle - ORC) and use solar radiation as an energy source.

### 6.1.3. Systems for converting solar energy into cold

The accompanying figures show some schematics of refrigeration plants that use solar radiation as an energy source.

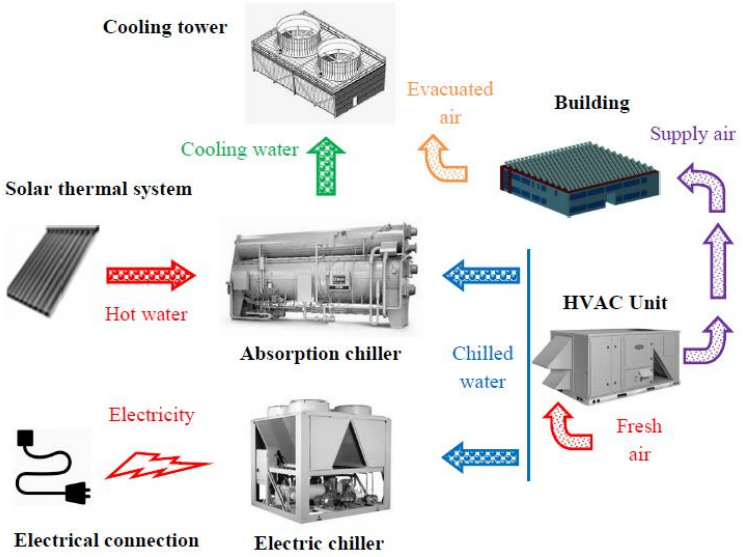

Diagram of a solar air conditioning system (Abrudan et al., 2019)

The use of solar energy for the production of cold (air conditioning, commercial cold, or industrial cold), contributes to increasing the efficiency of these installations, because it allows the reduction of electricity consumption.

### 6.1.4. Solar cogeneration systems

The adjacent figure shows the diagram of a cogeneration plant that uses solar radiation as an energy source.

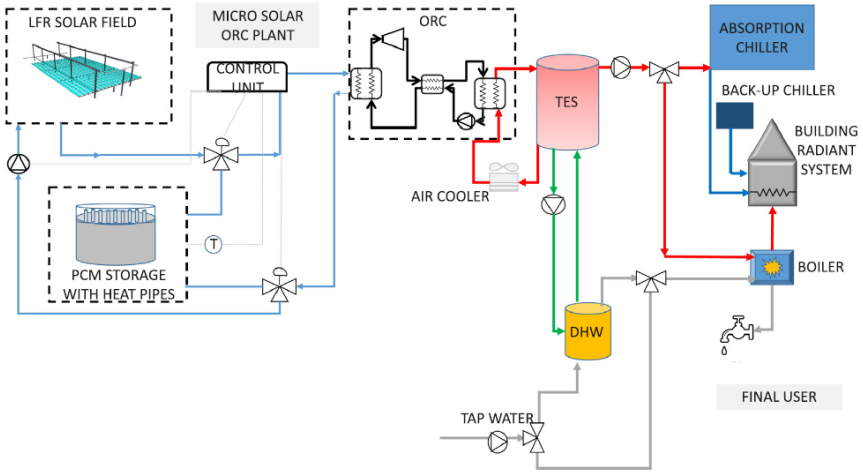

Trigeneration solar plant that produces
heat, electricity with an ORC system and cold with an absorption chiller
The solar system is based on collectors with linear concentrators (Fresnel) (Arteconi et al., 2019)

These cogeneration systems, which use solar energy for the combined production of electricity and heat, and sometimes also cold, represent only a few technological possibilities for integrating solar energy in such installations.

## 6.2. Solar energy conversion possibilities

In principle, the energy from the Sun, in the form of radiation and generically called "solar energy", can be converted into various forms of usable energy: heat, cold or electricity.

*The transformation of solar radiation into heat*can be realized in thermal solar collectors (or panels). In them, the heat is transported with the help of thermal agents, namely water, antifreeze, etc.).

*The transformation of solar radiation into electricity*can be realized in photovoltaic collectors (or panels). In these, electricity is produced by the photovoltaic effect.

*The transformation of heat into electricity*, can be achieved through the Rankine cycle. The working agent can be water (or steam), if the temperature of the heat source is high enough (over 300) °C, or a so-called organic agent, if the temperature of the heat source is low (50-300) °C. The name of the cycle is consistent with the nature of the working agent: steam Rankine cycle (Steam Rankine Cycle - SRC), or organic Rankine cycle (Organic Rankine Cycle - ORC).

*The transformation of heat into cold*, can be achieved through a particular refrigeration cycle, which uses heat, not electricity, as an energy source.

## 6.3. Solar radiation considerations

Considering that the distance between the Earth and the Sun is variable during the year, because the trajectory of the Earth around the Sun is an ellipse, and the intensity of solar radiation, which reaches the extreme of the atmosphere, is variable throughout the year, these variations being approx. ±3% of the solar constant value. This dependence on can determine with the following relation (Duffie, Beckman, 1980):

$$I_i = I_S \cdot \left(1 + 0.033 \cdot \cos\frac{360 \cdot n}{365}\right) \left[W / m^2\right]$$

where

n is the number of the day of the year.

## 6.4. The potential of using solar energy in Romania

Romania presents a relatively high potential for the use of solar energy. The energy contained in solar radiation reaches over 1400 kWh/m2/year, in the Black Sea area or in some southern regions, and in most of the rest of the country it reaches over (1250...1350) kWh/m2/year.

## 6.5. Notions of "solar geometry"

### 6.5.1. Theoretical considerations

For various applications where the use of solar energy is desired, it is important to study the relative position between the Earth and the Sun.

Several mathematical algorithms can be used to calculate the position of the Sun in the sky, including (Duffie & Beckman, 1980) or (Quaschning, 2007). Such an algorithm is presented in(Pop et al., 2021).

The location for which the calculations are made, is defined bylatitude (φ) and longitude (λ).

Next, the mathematical model is presented synthetically.

### 6.5.2. Results for Galati

Below are presented for the town of Galati and for several days of the year, the variation curves of the angle of incidence of solar radiation on the inclined surface, both depending on the angle of the solar

azimuth and depending on the solar time. The reference surface is considered characterized by γt=45°. The considered values of the angle of orientation with respect to the azimuth are: αt=0°, αt=90°, and αt=0°.

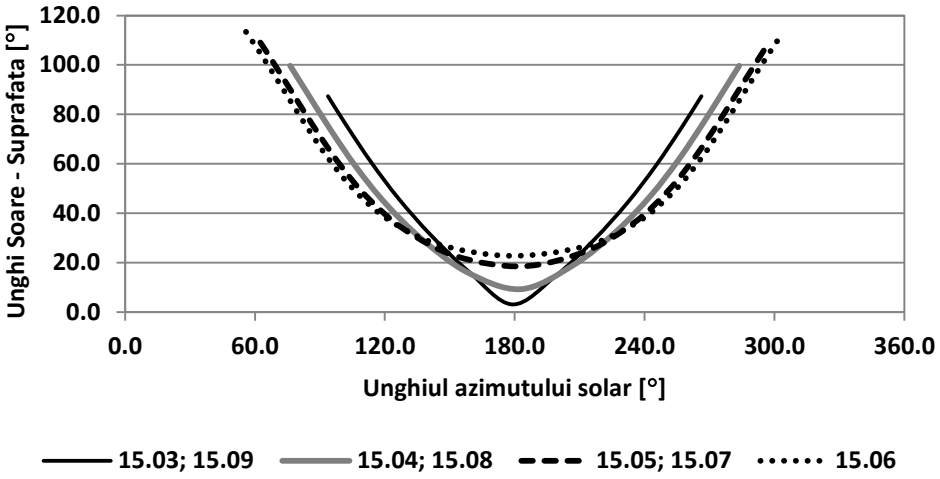


The curve of variation of the angle of incidence of solar radiation on the inclined surface depending on the solar azimuth angle
Galatians; (γt=45°); (αt=0° / South)

For the inclined surface facing South, the angle of incidence shows the lowest values when αs=180°, for which solar time is 12:00.

## 6.6. Solar radiation on inclined surfaces

### 6.6.3. Results for Galati

The figures below show for the town of Galati, the variation curves of the intensity of the global solar radiation in the horizontal plane incident on a surface inclined at 45° from the horizontal in the period (10-20).03 and in the period (10-20) .06.

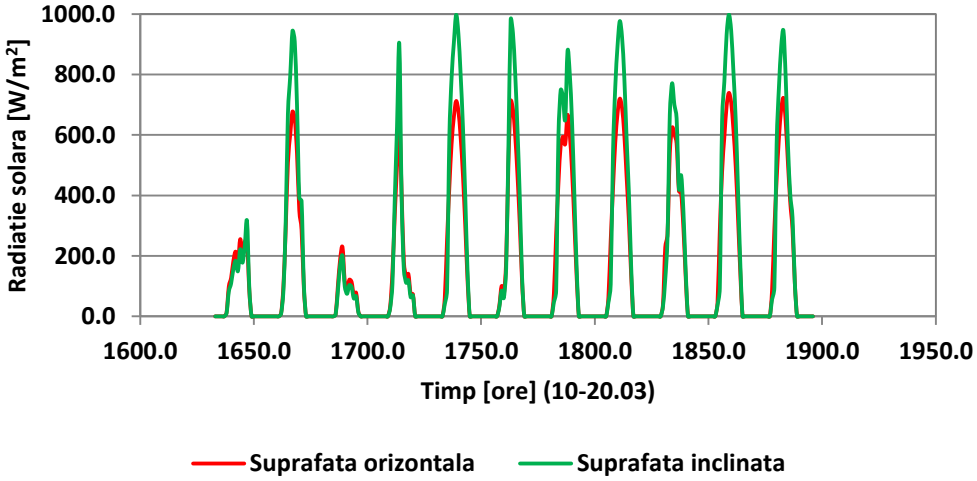


Variation curve of solar radiation intensity on horizontal and inclined surface during the period 10-20.03
Galatians; (γt=45°); (αt=0° / South)

It is observed that in March, the effect of the surface tilt is more pronounced than in June. At times, the effect of the surface tilt can be negative.

Such calculations can be performed for surfaces oriented to any cardinal point and inclined at any angle to the horizontal.

## 6.7. Efficiency of solar thermal collectors without concentrators

### 6.7.2. Results for Galati

Next, the variation of some characteristic parameters for a flat collector and for a collector with evacuated tubes, in the climatic conditions characteristic of the Galati locality, is presented. It is considered that $\gamma t = 40°$ and that $\alpha t = 0°$.

The figure below shows the variation curves for the thermal efficiency.

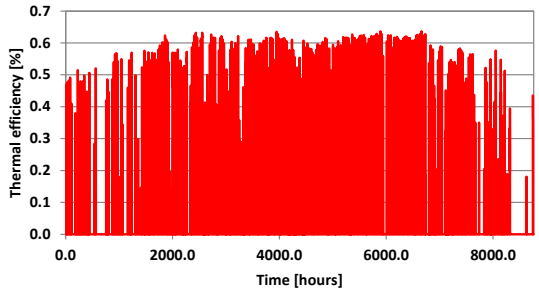


Variation curve of the thermal efficiency of the flat collector

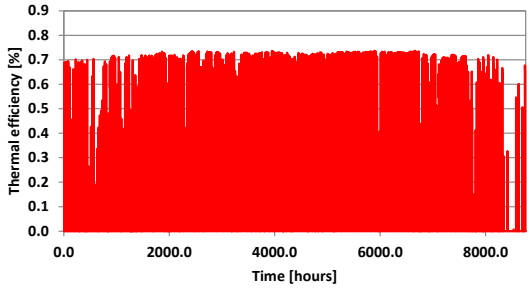


Variation curve of the thermal efficiency of the collector with evacuated tubes

## 6.8. The yield of thermal solar collectors with concentrators

### 6.8.4. Results for Galati

Below are presented the results obtained for a collector with the optical efficiency $\eta 0 = 0.8$ and the correction coefficient characteristic of thermal losses k1 = 0.64 W/m2K. All results are obtained for the municipality of Galati. The thermal regime of the diathermic oil in the collector receiver with parabolic concentrator is considered (370-390) °C.

The adjacent figure shows the variation curves of the projection of the solar altitude angle in the transverse plane of the collector ($\gamma St$), for one day from the middle of each month of the year.

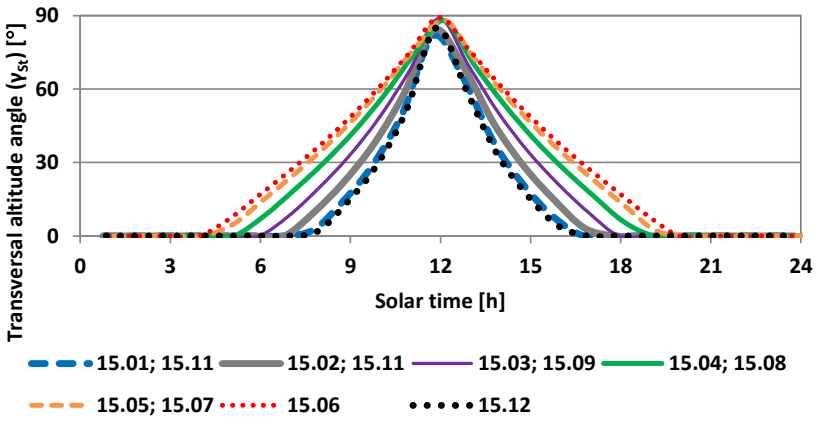


Variation curves of the solar altitude angle in the transverse plane of the collector

# 7. PRODUCTION OF COLD FROM SOLAR ENERGY

## 7.1. Introduction

The study presented below represents a collaboration between several universities in the country and one in Morocco and was carried out on the basis of an analytical model capable of highlighting the thermal behavior of all the elements of a solar absorption refrigeration system with hydro-ammonia solution. The energy source is represented by collectors with parabolic troughs, which serve different types of cold storage for food products: refrigerating room, refrigerated storage, freezing room and frozen storage. The types of heat demand considered for each refrigerated space investigated are: the heat accumulated through the walls, the heat accumulated through ventilation (fresh air), the technological cooling load (necessary for cooling the products) and the heat released during operation. The considered cooling installation is of the absorption type with NH3-H2O in one step, the energy source being represented by solar collectors with parabolic troughs, and the heat removal is carried out with water in a closed circuit with a cooling tower. For periods with insufficient solar energy, a classic one-stage mechanical compression cooling plant with NH3 as refrigerant is considered and dimensioned as alternative equipment. The effect of seasonal thermal storage on the behavior of the system is also investigated, it being dimensioned in such a way as to reduce as much as possible the need to use the installation with mechanical compression.

## 7.2. Material

The principles of the study are generally valid, but have been applied to a case study that considers the location Seville in Spain, respectively the coordinates 37.094 N and 2.358 E. According to the Köppen-Geiger classification (Köppen, 1936), Seville is in the Mediterranean climate with hot summers (Csa). The climatic data taken into account for the calculations were taken from the typical meteorological year (TMY – Typical Meteorological Year), available on the website of the European Union, which provides hourly variations of several climatic parameters: dry bulb temperature (or ambient temperature) (tdb [°C]), relative humidity (φ [%]), global solar radiation on the horizontal surface (I [W/m2]), direct normal radiation (Idir or DNI [W/m2]), etc. Other locations with high solar potential may also be considered for such studies.

For the sake of simplicity, for this study, all types of cold storage, considered as food storage facilities, were considered to be for chicken meat. The influence of other products can also be investigated. The dimensions considered for all four cold spaces are:

- For RS and FS: length 50 m, width 20 m and height 5 m
- For RC and FC: length 3 m, width 2 m and height 2.5 m

For all the cooled spaces, every wall, ceiling and floor was considered to be made of sandwich panels filled with polyurethane. The thickness of these panels was calculated based on an ambient temperature of 40 °C and a relative humidity of 40%.

The indoor temperature was considered to be 3 °C for refrigeration and -20 °C for freezing. The indoor relative humidity was assumed to be 90% in all cases.

The air flow rate for ventilation was considered to be 3 shifts in 24 hours (15000 m3/h).

Some more modern models of SPTC are available in the market, but in this study, the aforementioned model was preferred, due to the availability of experimental data presented in (Dudley et al., 1994).

The alternative refrigeration equipment, to be used in periods without the existence of solar heat, is a classic one-stage mechanical refrigeration apparatus with ammonium as the refrigerant. To increase the existence of solar heat, a heat accumulator was proposed and its influence was investigated.

A closed circuit cooling tower is used to remove heat from both the thermal plant (by absorption) and the electric machine (by mechanical compression).

The principle diagram of the investigated system is shown in figure 1.

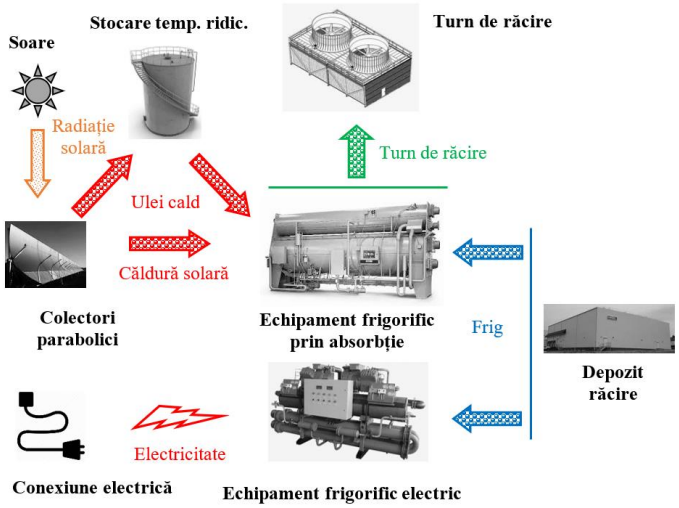


Fig. 1. Schematic diagram of solar absorption cooling system with reciprocating electrical installation

It can be seen that the cold can be extracted from the cold storage spaces both by the absorption plant, with operation based on solar heat, and by the mechanical plant, operated electrically. The thermal behavior and energy exchanges of both refrigeration systems were investigated.

## 7.3. Method

### 7.3.1. Time variation of the cooling load transmitted through the walls

The time variation of the cooling load (or thermal power) transmitted through the walls is determined by the variation of the ambient temperature. The dependence of this type of cooling load on the ambient temperature is linear.

The cooling load through the walls () can be determined with equation 1:$\dot{Q}_w$[W]

$$\dot{Q}_w = k \cdot S \cdot (t_{db} - t_i)\ [W] \quad (1)$$

where:

k·S [W/K] is the thermal characteristic of cold storage spaces
tdb [°C] is the variable dry bulb temperature (ambient temperature)
ti [°C] is the internal temperature of the cold storage spaces (3 °C for RC and RS respectively -20 °C for FC and FS)

The values (k·S) for cold storage spaces are shown in table 4.

Table 4. Values (k·S) for cold storage spaces

| **Deposit type** | **r** | **r** | **FC** | **FS** |
|---|---|---|---|---|
| (k·S) [kW/K] | 0.0135 | 0.676 | 0.0083 | 0.50 |

These values depend on the insulation level of each wall and the dimensions of the warehouse.

The cooling load through the walls () can also be determined with equation 2:$\dot{Q}_w$[W]

$$\dot{Q}_w = \frac{\dot{Q}_n}{t_n - t_i} \cdot t_{db} - \frac{\dot{Q}_n \cdot t_l}{t_n - t_i} \; [W] \quad (2)$$

where:

$\dot{Q}_n$[W]is the nominal cooling load through the walls, determined under nominal working conditions (0.5 kW for RC, 25 kW for RS, 0.5 kW for FC and 30 kW for FS)
tn = 40 °C is the nominal dry bulb temperature considered in this study

### 7.3.2. Time variation of cooling load due to ventilation

The only refrigerated storage space with ventilation is RS, and the cooling load due to ventilation is determined by the need to cool fresh air from the variable ambient temperature to the indoor temperature.

The cooling load due to ventilation () can be calculated with equation (3):$\dot{Q}_v$[W]

$$\dot{Q}_v = \rho \cdot \dot{V} \cdot c \cdot (t_{db} - t_i) \; [W] \quad (3)$$

where:

ρ [kg/m3] is the density of fresh air
$\dot{V}$[m3/s] is the fresh air volume flow rate calculated to provide 3 air changes in 24 hours
c [kJ/kgK] is the specific heat of fresh air

### 7.3.3. Time variation of technological cooling load

The time variation of the technological cooling load was considered based on the cooling load curve shown in (Davey and Pham, 2014).

To calculate the technological cooling load () in the case of chicken meat storage, the time variation (τ [h]) was taken into account using the proposed equation:$\dot{Q}_t$[W/kg]

$$\dot{Q}_t = a \cdot \tau^2 - b \cdot \tau + c \quad (4)$$

The total amount of cold calculated for refrigerating 1 kg of chicken meat was 64.8 Wh/kg, compared to the value of 60.0 Wh/kg corresponding to the enthalpy change over 10 hours. The calculated value represents an overestimation of 8.0 %. The total amount of cold calculated for freezing 1 kg of chicken meat was 176.4 Wh/kg. Compared to the value of 180.0 Wh/kg corresponding to the enthalpy change in 20 hours. The calculated value represents an underestimation of 2.0 %.

To the author's knowledge, such an equation is not available in the specialized literature.

Similar variations in technological cooling load can be determined for other categories of food or non-food products.

### 7.3.4. Time variation of cooling load due to operation

The cooling load due to the operation, represents the heat penetrations through the operations of loading, unloading, etc.

In this study, the cooling load due to operation () was determined as a part of the cooling load through the walls with equation (5):$\dot{Q}_{op}$ $[W]$

$$\dot{Q}_{op} = 0.4 \cdot \dot{Q}_w \quad (5)$$

### 7.3.5. The analytical model for the efficiency of parabolic trough collectors

The location is determined by longitude (λ [°]) and latitude (φ [°]), while the position of the sun is defined by the solar altitude angle (γS [°]) and solar azimuth angle (αS [°]). The orientation of the collectors is defined by the tilt angle (γt [°]) and the azimuth related orientation angle (αt [°]).

The solar angle of incidence on the inclined surface of the SPTC (θ [°]) and the global thermal efficiency of the SPTC (η [-]), were calculated using the analytical model presented and validated in(Zaoumi et al., 2021). Some information about SPTC is also presented in (Pop et al., 2021).

### 7.3.6. The thermal regime of the cooling tower

Investigating the thermal regime of the cooling tower during the whole operating period of the year is important, because this equipment is used by both types of refrigeration plants: the solar absorption plant and the electrically operated plant used as a backup.

The cooling water temperature (returning from the cooling tower) was determined as a function of the wet bulb temperature (twb [°C]):

$$t_w = t_{wb} + 5\ [°C] \tag{6}$$

The difference of 5 °C is consistent with (Syed et al., 2005) where this temperature difference, for such applications, is reported in the range of (3.2 – 4.8) °C, and consistent with (Stanford III, 2003) where this temperature difference is reported in the range (1.5 – 5.5) °C.

In turn, the wet bulb temperature is determined by the ambient temperature (dry bulb temperature) (tdb [°C]) and the relative humidity (φ [%]) of the ambient air, and was calculated using the equation shown in (Stull, 2011):

$$t_{wb} = t_{db} \cdot atan\left[0.151977 \cdot (\varphi + 8.313659)^{1/2}\right] + atan(t_{db} + \varphi) - \\ - atan(\varphi - 1.676331) + 0.00391838 \cdot \varphi^{3/2} \cdot atan(0.023101 \cdot \varphi) - 4.686035 \tag{7}$$

The operation of the cooling tower was considered variable, to maintain a minimum exit cooling water temperature of 10 °C. Thus, if the ambient temperature drops, the fan speed will be reduced to maintain the minimum set cooling water temperature.

### 7.3.7. Thermal behavior of the storage tank

The storage tank is filled with diathermic oil and acts as a heat accumulator to serve the plant by absorption during periods of low or no solar radiation. The tank is heated when excess solar radiation is available and cooled when the stored heat is used.

The temperature variation of the oil in the storage tank (Δt [°C]) in a period (τ [s]), can be determined as a function of the heat exchanged (Qst [kJ]):

$$\Delta t = \frac{Q_{st}}{m \cdot c} \tag{8}$$

where:

- m [kg] is the mass of the oil in the storage tank
- c = 1.85 kJ/kgK is the average specific heat of the oil.

The heat exchanged can be calculated from the heat balance on the storage tank:

$$Q_{st} = Q_{sol,ex} - Q_{op,st} - Q_{loss} \tag{9}$$

where:

- Qsol,ex [kJ] is the excess solar heat (exceeding the heat required for the operation of the installation by absorption)

- Qop,st [kJ] is the heat required for operation and extracted from the storage tank for plant operation by absorption
- Qloss [kJ] is the heat lost through the insulation of the storage tank under the variable temperature difference between the oil and the outside air.

A polyurethane thermal insulation layer with a thickness of 0.5 m was considered.

### 7.3.8. Absorption refrigeration plant

The schematic diagram of the NH3-H2O single-stage absorption refrigeration plant is shown in figure 6.

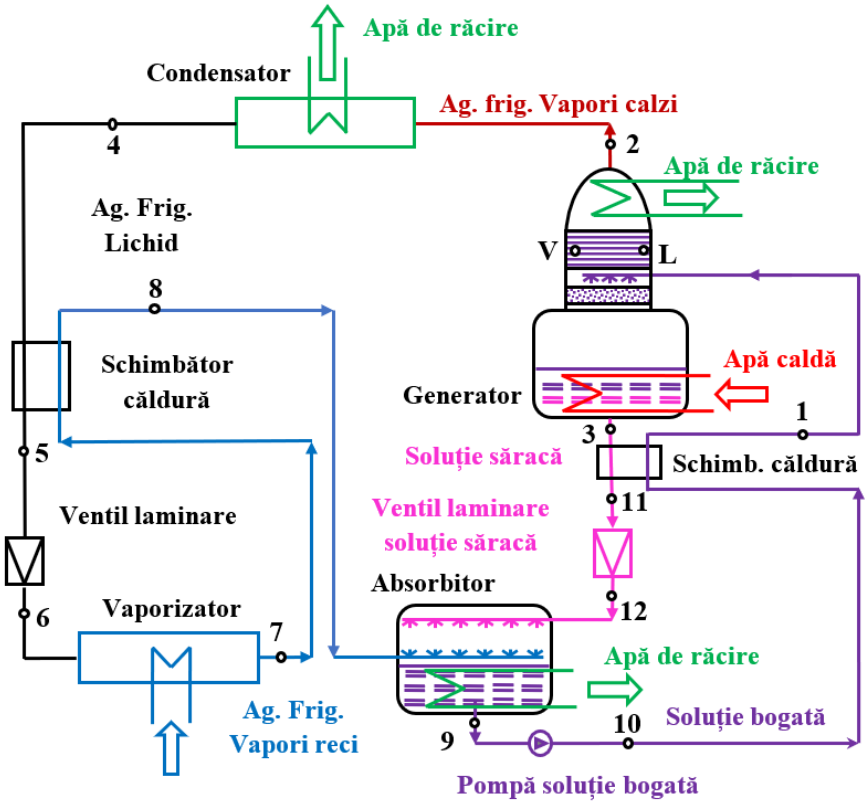


Fig. 6. Schematic diagram of the NH3-H2O absorption refrigeration plant

The main refrigeration circuit is composed of condenser, laminator, evaporator and heat exchanger, while the thermochemical compressor consists of the following components: absorber, rich solution pump, vapor generator, concentrate solution laminator and heat exchanger . The refrigerant is NH3 and the solvent is H2O.

Internal working conditions were determined by external working conditions.

The vaporization temperature (t0 [°C]) was determined as a function of the indoor temperature (ti [°C]):

$$t_0 = t_7 = t_i - 13\ [°C] \tag{10}$$

The assumption that the vapors of the refrigerant at the exit from the evaporator are at the vaporization temperature is consistent with (Sun, 1996). The vaporization temperature determines the vaporization pressure (p0 [bar]).

The condensing temperature (tk [°C]) was determined as a function of the cooling water temperature (tw [°C]) on the cooling tower return:

$$t_k = t_4 = t_w + 8\ [°C] \tag{11}$$

The assumption that the liquid refrigerant at the outlet of the condenser is saturated is consistent with (Bulgan, 1994). The condensing temperature determines the condensing pressure (pk [bar]).

The temperature of the saturated lean solution at the generator exit (tg [°C]) was determined as a function of the hot oil temperature (th [°C]) on the solar system return:

$$t_g = t_3 = t_h - 10\ [°C] \tag{12}$$

The difference of 10 °C is consistent with (Alvarez and Trepp, 196).

The temperature of the superheated refrigerant (t8 [°C]), at the exit of the heat exchanger in the main refrigerant circuit, was determined as:

$$t_8 = t_k - 20\ [°C] \tag{13}$$

The enthalpy of the subcooled refrigerant (h5 [kJ/kg]) at the exit of the heat exchanger from the main refrigerant circuit, was determined from the energy balance equation on the heat exchanger

$$h_5 = h_4 - h_8 + h_7 [kJ/kg] \tag{14}$$

The enthalpy at the outlet of the lamination valve on the main refrigerant circuit (h6 [kJ/kg]) is equal to the enthalpy at its inlet:

$$h_6 = h_5 [kJ/kg] \tag{15}$$

The parameters of the saturated vapor of the refrigerant at the exit from the generator (state 2) were determined at the condensing pressure (p2 = pk) and temperature (t2 = tk).

The parameters of the saturated lean solution, at the exit from the generator (state 3) were determined at the condensing pressure (p3 = pk) and at the temperature at the exit of the generator (t3 = tg).

The parameters of the saturated rich solution at the outlet of the absorber (state 9) were determined at the vaporization pressure (p9 = p0) and the condensation temperature (t9 = tk).

The enthalpy of the rich solution at the exit of the pump (state 10) was determined as a function of the specific mechanical work of the pump (wP [kJ/kg]) as:

$$h_{10} = h_9 + w_P [kJ/kg] \tag{16}$$

with

$$w_P = \Delta p \cdot v_9 [kJ/kg] \tag{17}$$

where (Δp = pk – p0) and v9 [m3/kg] is the specific volume of the rich solution at the pump inlet.

The parameters of the saturated rich solution in the generator concentration column (state L) were determined at the condensing pressure (pL= pk) and the concentration of the rich solution.

The parameters of the saturated vapor in equilibrium with the rich solution in the generator concentration column (state V) were determined at the condensing pressure (pV= pk) and the equilibrium temperature of the rich solution and vapor (tV = tL).

The temperature of the subcooled rich solution at the generator inlet (t1 [°C]) was determined as a function of the temperature of the saturated liquid (state L):

$$t_1 = t_L - 3\ [°C] \tag{18}$$

The recirculation factor (f [-]), representing the ratio between the flow of the rich solution () and the flow of the refrigerant in the main refrigeration circuit (), was determined according to the

concentrations of NH3 in the main refrigeration circuit (ξ"=1), from the circuit of rich solution (ξr) and from the circuit of lean solution (ξw):$\dot{m}_r$ $[kg/s]\dot{m}$ $[kg/s]$

$$f = \frac{\xi" - \xi_w}{\xi_r - \xi_w} = \frac{1 - \xi_w}{\xi_r - \xi_w} \quad (19)$$

where (ξw = ξ3) and (ξr = ξ9).

The enthalpy of the subcooled lean solution at the entrance to the lamination valve (h11 [kJ/kg]), was determined from the energy balance equation on the heat exchanger on the NH3-H2O circuit:

$$h_{11} = h_3 - \frac{f}{f-1} \cdot (h_1 - h_{10})[kJ/kg] \quad (20)$$

The enthalpy at the exit from the lamination valve on the lean solution circuit (h12 [kJ/kg]) is equal to the enthalpy at the entrance to it:

$$h_{12} = h_{11}[kJ/kg] \quad (21)$$

The enthalpy of the ideal rectification pole (hPi [kJ/kg]) was determined as a function of the enthalpies (hL [kJ/kg]) and (hV [kJ/kg]), and the concentrations in NH3 (ξL [kJ/kg]) and V (ξL [kJ/kg]) in the L and V states, respectively:

$$h_{Pi} = \frac{h_V \cdot (1 - \xi_L) - h_L \cdot (1 - \xi_V)}{\xi_V - \xi_L} \quad (22)$$

The specific heat output of the absorber (qAB [kW/kg]) was determined from the energy balance on the absorber:

$$q_{Ab} = h_8 + (f - 1) \cdot h_{12} - f \cdot h_9 \quad (2.\ 3)$$

The specific heat output of the ideal rectifier (qRi [kW/kg]) that should be discharged from the rectifier (located at the top of the generator concentration column), was calculated as:

$$q_{Ri} = h_{Pi} - h_2 \quad (24)$$

The specific thermal power of the actual rectifier (qR [kW/kg]) was determined considering a rectification efficiency (ηr = 0.88):

$$q_R = \frac{q_{Ri}}{\eta_r} \quad (25)$$

The specific heat output of the generator (qG [kW/kg]) was determined from the energy balance of the generator:

$$q_G = q_R + (f - 1) \cdot h_{12} - f \cdot h_9 \quad (26)$$

The specific heat capacity of the condenser (qk [kW/kg]) was determined from the energy balance of the condenser:

$$q_k = h_2 - h_4 \quad (27)$$

The specific heat output of the vaporizer (q0 [kW/kg]) was determined from the energy balance on the vaporizer:

$$q_0 = h_7 - h_6 \quad (28)$$

The coefficient of performance (COP [-]) was determined as the ratio between the specific heat powers of the evaporator and the generator:

$$COP = \frac{q_0}{q_G} \quad (29)$$

The heat outputs of all equipment were determined by multiplying the specific heat outputs with the mass flow rates corresponding to each equipment.

### 7.3.9. High temperature limits at the exit of the solar system

The working conditions of the absorption refrigeration plant are determined by the temperatures of the three heat sources:

- Internal temperatures of storage spaces (ti[°C])
- Cooling water temperature leaving the cooling tower (tw [°C])
- Heat medium temperature at SPTC outlet (also called high temperature) (th [°C]).

In this study, the thermal agent in the solar system circuit was considered a diathermic oil, used in turn to prepare hot water, used in the steam generator.

It was considered that during operation, the internal temperatures of the storage spaces were constant (3 °C for RC and RS respectively -20 °C for FC and FS).

Since the temperature of the cooling water is variable under the influence of ambient conditions (tdb and φ), the temperature of the hot diathermic oil must be adjusted to maintain a minimum degassing area (Δξ), representing the difference between the concentrations of the rich solution (ξr) and the lean solution (ξw ):

$$\Delta\xi = \xi_r - \xi_w \tag{30}$$

A minimum degassing area must be maintained because if the degassing area decreases too much, the flow rates of lean and rich solutions increase greatly.

The elevated temperature was determined for both refrigeration and freezing, considering two minimum values of the degassing zone (Δξ = 0.06) and (Δξ = 0.1).

The correlation between COP and cooling water temperature, for NH3 as refrigerant, was determined as:

$$COP = e \cdot t_w^2 + f \cdot t_w + g \tag{33}$$

with values of coefficients e, f and g, shown in table 10.

Table 10. Values of coefficients e, f and g (eq. 33)

| Regime | e | f | Mr |
|---|---|---|---|
| Refrigeration (t0 = -10 °C) | 0.0034 | -0.2724 | 8.3136 |
| Freezing (t0 = -30 °C) | 0.0009 | -0.0863 | 3.9280 |

The correlation shown with the calculated coefficients was used to determine the COP of the backup mechanical refrigeration plant, required to be used when solar heat is absent or insufficient.

The presented mathematical model characterizes the thermal behavior of all the investigated components of the solar cooling system: the cold spaces (RC, RS, FC, FS), the food product itself (chicken), the collectors with parabolic troughs, the cooling tower, the main system absorption cooling and the back-up mechanical cooling system.

Different variants of the mathematical model (depending on the type of cooled space) were implemented in Engineering Equation Solver (EES) and in Microsoft Excel.

## 7.4. Results and discussion

The location in Seville was chosen to highlight the computational capabilities of the mathematical model. Separate case studies were conducted for each type of chilled space: RC, RS, FC and FS. The full results of the study are presented in (Balan et al., 2021).

### 7.5. Conclusions

The study presents a new perspective on the analytical investigation of food product cooling with hydro-ammonia solution solar absorption cooling systems served by parabolic trough solar collectors. From the author's knowledge, the study investigates the following new aspects, which are not addressed in the specialized literature:

- Cooling food products with a solar absorption cooling system,
- Modeling with hourly time step, for long periods of time, the variation of the thermal load required for cooling food products,
- Long time hourly time step variation of NH3-H2O absorption solar system performance.

Following the detailed presentation of the proposed mathematical model, a case study for Seville is presented.

The thermal behavior of four types of cold spaces: RC, RS, FC and FS and of solar heat accumulators were investigated, considering two types of values (low and high) of the storage temperature, considered as an important functional parameter of these systems .

The considered configurations of the solar cooling system consisted of different numbers of SPTCs: 1, 2, 4, 6, 8, 10 and 12, and different volumes of storage tanks: 1, 10, 20, 50, 100, 200,500, 1000, 3000, 5000 and 10000 m3.

## 8. FINAL CONCLUSIONS AND PERSONAL CONTRIBUTIONS

## 8.1. Final conclusions

Inscribed on the trajectory of achieving the goal of ensuring an environment with zero greenhouse gas emissions, the doctoral thesis addresses several topics of utmost importance:

a) Increasing the efficiency of processes and systems for the production of electricity, heat and cold;
b) Reducing methane emissions from solid household waste storage fields;
c) Optimization analysis of solar energy concentrators;
d) Highlighting the availability of solar energy on the territory of Romania;
e) The study of the optimization of cold and heat production using solar energy as a thermal resource.

In the analysis of the processes and systems for the production of electricity, heat and cold, the doctoral thesis calls for an innovative strategy based on the exergetic method, the only one that makes the connection between the system and its environment in which it evolves. Exergetic analysis manages to penetrate the boundary separating the system from its external environment and highlight the location and extent of usable energy consumption due to the internal irreversibility of functional processes. The reduction of these consumptions will be the strategy to follow in order to find the optimal functional regimes and the optimal constructive structures.

The paper summarizes the problem of calculating the relative position between the sun and the plane of the collectors, but also the efficiency of energy conversion from solar radiation into heat with flat collectors, but also with radiation concentrators, especially with parabolic troughs, with the presentation of calculation examples for the town of Galati. The variations of some geometric parameters, the intensity of solar radiation incident on its components, the efficiency of the collectors or the specific thermal power of the collectors were determined.

Regarding the chapter on the cooling with the help of solar energy of a cold store for food products, several important conclusions were drawn.

The study presents a new perspective on the analytical investigation of food product cooling with hydro-ammonia solution solar absorption cooling systems served by parabolic trough solar collectors. From the author's knowledge, the study investigates the following new aspects, which are not addressed in the specialized literature:

- Cooling food products with a solar absorption cooling system,
- Modeling with hourly time step, for long periods of time, the variation of the heat load required for cooling food products,
- Hourly time-step variation of NH3-H2O absorption solar system performances over long periods of time.

Following the detailed presentation of the proposed mathematical model, a case study for Seville is also presented.

The thermal behavior of four types of cold spaces: RC (refrigeration cooling), RS (refrigeration storage), FC (freezing cooling) and FS (frozen storage) and of solar heat accumulators were investigated, considering two types of values (low and high) of the storage temperature, considered as an important functional parameter of these systems.

The considered configurations of the solar cooling system consisted of different numbers of SPTC collectors (solar parabolic thermal collectors): 1, 2, 4, 6, 8, 10 and 12, and different volumes of the storage tanks: 1, 10, 20 , 50, 100, 200,500, 1000, 3000, 5000 and 10000 m3.

Investigations carried out in the study revealed the following main findings:

- The solar cooling system cannot significantly reduce the maximum electrical power absorbed and therefore the investment in the backup electrical cooling plant. Further investigations should be conducted to analyze whether multiple SPTCs can lead to such performance.
- As the number of SPTCs increases, the total amount of solar heat available increases, and the volume of storage required to reduce or remove excess solar heat also increases.
- With 1 and 2 SPTC, the direct solar heat requirement is practically not exceeded, so in these situations the storage tank is not justified. For configurations with more than 4 SPTCs, the available solar heat increases significantly and the maximum storage temperature increases with the number of SPTCs and decreases with the size of the storage tank.
- With a small number of SPTCs (1 – 4), the amount of cold production directly from solar heat increases significantly with the number of SPTCs. As the number of SPTCs increases (especially at 8 – 12), the impact of the number of SPTCs decreases, due to the increasing amount of excess solar heat.
- As the number of SPTCs increases, so does the storage volume corresponding to maximum cold production from the stored heat. The value of the cold produced from the stored heat decreases at high values of the storage volume, because the temperatures of the stored oil decrease and thus become insufficient to supply the solar cooling plant for longer periods of time.
- It is difficult to achieve 100% of total solar cold production (directly from solar heat and from stored solar heat). In the cases considered, the following maximum values of the total solar cold production weights were reached: for RS 99.7%, for RC 99.4%, for FS 93.8% and for FC 78.7%.
- Higher values of total solar cold production can be achieved by increasing the number of SPTCs, but the energy efficiency increases faster with a reduced number of STPCs. For each configuration, an optimal storage tank size can be identified that ensures maximum energy efficiency. However, smaller tanks can be used to achieve high efficiencies in the vicinity of the maximum possible values.
- In the cases of 1 and 2 SPTC (for refrigeration) and in the cases of 1, 2 and 4 SPTC (for freezing), the amount of cold produced from electricity is constant, not being influenced by the size of the storage tank. In cases of more than 4 SPTCs, the minimum amount of cold produced from electricity decreases with the number of SPTCs, but corresponds to smaller

storage volumes rather than large storage volumes. For high storage temperatures, the sizes of the storage tanks corresponding to the lower shares of electricity-produced cold are smaller than for low storage temperatures.

- For all types of cold spaces considered, the highest electricity savings were achieved for 12 SPTC with the following storage tank volumes:
    - For low storage temperatures for RC: 500 m3, for RS and FC: 1000 m3 and for RS: 3000 m3;
    - For high storage temperatures for RC and RS: 50 m3, and for FC and RS: 500 m3.

## 8.2. Personal contributions

Among the original contributions of the thesis can be mentioned:

- The bibliographic study regarding the current state of research in the field, which points out the capital importance of the subject in which the thesis is thematic, namely that of reaching the level of economic and social development with zero greenhouse gas emissions, is an original contribution of the thesis;
- Highlighting on exergetic bases the real causes of the inefficiency of the separate production of electricity and heat and the presentation of solutions to reduce consumption in these systems, represents an original contribution of the thesis;
- For the modeling and simulation of the operation of energy systems for the production of electricity, cold and heat, original calculation programs are built based on which valuable and interesting original information was obtained regarding the influence of the decision-making parameters and the constructive structure of the systems on the real efficiency of the installations;
- The original exergetic analyzes developed in the thesis clearly highlight the advantages of cogeneration production of mechanical energy and heat or heat and cold;
- The thesis presents an original method for estimating the value of use (exergy) of solid household waste that can be used as fuel in systems that operate after engine cycles; the experimental analysis on the basis of which the compositions of different samples of household solid residues were determined and the technique of calculating their usable energy represents an original contribution of the thesis;
- The calculation of the relative position between the sun and some plane in which the conversion of solar energy into heat is carried out;
- The mathematical calculation model was created and the energy efficiency and thermal energy production of flat thermal solar collectors and with radiation concentrators were evaluated in the specific climatic conditions of Galati, respectively Seville;
- A mathematical model was developed for calculating the heat requirement of cold stores, taking into account wall losses, ventilation losses, technological requirements and operational losses;
- A complex mathematical model was developed for the calculation of refrigeration installations with hydro-ammonia solution;
- A heat accumulator was integrated into the refrigeration system based on solar energy, which would allow the operation of the cooling installation with heat from solar energy, for as long as possible;
- The behavior of the heat accumulator was investigated in two thermal regimes, one with the maintenance of the minimum temperature necessary for the operation of the refrigeration plant by absorption and one with the maintenance of the maximum temperature that can be ensured with the help of collectors with parabolic solar radiation concentrators;
- Mathematical modeling in transient regime of the solar refrigeration installation, with heat accumulator, was carried out in the specific climatic conditions for Seville;
- The performance and efficiency of various configurations were evaluated regarding the number of thermal solar collectors with parabolic troughs and the volume of the storage tank;

- Practical recommendations were made regarding the optimal configurations of the investigated solar refrigeration systems, both regarding the number of collectors and the recommended volumes for the storage tanks.

**Key words:** Exergy, Hot cold cogeneration, Municipal waste, Solar energy, Solar thermal collectors (SPTC), Collectors with Parabolic troughs.

## Bibliographical references

1. Aboelwafa O, Fateen SE.K, Soliman A, Ismail IM - A review on solar Rankine cycles: Working fluids, applications, and cycle modifications, Renewable and Sustainable Energy Reviews 82 (2018) 868–885
2. Abrudan AC, Pop OG, Serban A., Balan MC - New Perspective on Performances and Limits of Solar Fresh Air Cooling in Different Climatic Conditions, Energies 2019, 12, 2113
3. Alvares, SG, Trepp, Ch., 1987. Simulation of a solar driven aqua-ammonia absorption refrigeration system Part 1: mathematical description and system optimization. International J. Refrig. 10, 40-48.
4. Alvares, SG, Trepp, Ch., 1987. Simulation of a solar driven aqua-ammonia absorption refrigeration system Part 2: viability for milk cooling at remote Brazilian dairy farms. International J. Refrig. 10, 70-76.
5. ANRE - National Report 2016 https://www.anre.ro/download.php?f=hKh%2Fgg%3D%3D&t=vdeyut7dlcecrLbbvbY%3D
6. Balan MC, Jäntschi L., Bolboacă SD, Damian M. - Thermal Solar Collectors Behavior in Romania, Polish Journal of Environmental Studies, ISSN 1230-1485, 2010, 19(1):231-241
7. Balan, M., Pop, OG, Dobrovicescu, A., Serban, A., Ciocan, M., Zaaoumi, A., Hiris, DP (2021). Analytical modeling of food storage cooling with solar ammonia-water absorption system, powered by parabolic trough collectors and with case studies for Seville, Mendeley Data, V2, doi: 10.17632/h95284fmgf.2
8. Behar O. - Solar thermal power plants – A review of configurations and performance comparison, Renewable and Sustainable Energy Reviews 92 (2018) 608–627
9. Bejan, A., Tsatsaronis, G., Moran, M., Thermal Design and Optimization, Wiley, New York, 1996;
10. Bilgen, E., Takahashi, H., Exergy analysis and experimental study of heat pump system, Exergy, An Int. J. 2002, 2(4). pp. 259-65.
11. Borel, L., Favrat, D. Thermodynamics and Energy Systems Analysis: From Energy to Exergy. EPFL Press (2010)
12. Boumanchar I., Chhiti Y., Alaoui FEM, Ouinani AE, Sahibed-Dine A.,, Bentiss F., Jama C., Bensitel M., Effect of materials mixture on the higher heating value: Case of biomass, biochar and municipal solid waste, Waste Management, March 2017, Volume 61, pp. 78-86;
13. **Ciocan M.**, Dobrovicescu A.,Serbian A.,Stefanescu M.-F.,Nastase G., Comparative energetic and exergetic analysis of individual or cogenerative systems with steam turbines for producing heat and mechanical work,19th International Multidisciplinary Scientific GeoConference SGEM 2019, 30 June - 6 July, 2019, pp. 109-116,ISBN:978-619-7408-88-1, DOI:10.5593/sgem2019/6.1/S24.014
14. De Luca F., Ferraro V., Marinelli V. - On the performance of CSP oil-cooled plants, with and without heat storage in tanks of molten salts, Energy 83 (2015) 230-239
15. Dincer, I., 2003. Refrigeration Systems and Applications. John Wiley & Sons, Ltd., Chichester.
16. Dobrovicescu, A., Exergetic and exergoeconomic analysis of refrigeration and cryogenic systems, AGIR, Bucharest, 2000;
17. Dobrovicescu, A., Exergetic analysis of a cryogenic refrigeration system, The 18th International Conference on Efficiency, Cost, Optimization, Simulation and Environmental

Impact of Energy Systems "Shaping our future energy systems" ECOS 2005, Trondheim, Norway, 2005, 345-352 ;
18. Dobrovicescu, A., Tsatsaronis, G., Exergy destruction due to friction in heat exchangers – A refrigeration system case study, ECOS 2006, p. 165-173
19. Dudley V., Colb GJ, Sioan M., Kearney D. - Test results. SEGS LS-2 solar collector, SAND, 1994
20. Duffie J., Beckman WA, Solar engineering of thermal processes, Second edition, John Wiley & Sons, Singapore, 1980
21. El Fadar, A., Mimet, A., Pérez-García, M., 2009. Modeling and performance study of a continuous adsorption refrigeration system driven by parabolic trough solar collector. Soil. Energy 83, 850-861.
22. Geyer M., Lüpfert E., Osuna R., Esteban A., Schiel W., Schweitzer A., Zarza E., Nava P., Langenkamp J., Mandelberg E. - EUROTROUGH - Parabolic Trough Collector Developed for Cost Efficient Solar Power Generation, 11th Int. Symposium on Concentrating Solar Power and Chemical Energy Technologies, September 4-6, 2002, Zurich, Switzerland
23. Ghorbani, B., Mehrpooya, M., 2020. Concentrated solar energy system and cold thermal energy storage (process development and energy analysis). Sustainable Energy Technol. Assess. 37, 100607.
24. Giostri A., Binotti M., Silva P., Macchi E., Manzolini G. - Comparison of two linear collectors in solar thermal plants: parabolic trough vs FRESNEL, Proceedings of the ASME 2011 5th International Conference on Energy Sustainability ES2011 August 7- 10, 2011, Washington, DC, USA
25. Giostri A., Binotti M., Astolfi M., Silva P., Macchi E., Manzolini G. - Comparison of different solar plants based on parabolic trough technology, Solar Energy 86 (2012) 1208–1221
26. Goswami, DY, 2015. Principles of solar engineering, third ed. Taylor & Francis, Boca Raton.
27. Grosu, L. Contribution al′optimisation thermodynamique et economique des machines a cycle inverse a deux et trois reservoirs de chaleur. Ph.D.Th, Institut National Polytechnique de Lorraine (2000) France.
28. Gueymard, CA, Myers, D., Emery, K., Proposed reference irradiance spectra for solar energy systems testing, Solar Energy 73(6), pp. 443–467, 2002
29. Halkos G. and Petrou KN,*Analyzing the Energy Efficiency of EU Member States: The Potential of Energy Recovery from Waste in the Circular Economy*,Energies, 2019, 12(19), 3718;https://doi.org/10.3390/en12193718;
30. Kalogirou SA - Detailed thermal model of a parabolic trough collector receiver, Energy 48 (2012) 298-306
31. Kousskou, T., Dobrovicescu, A., Gibout, S., Strub, F., Comparaison de méthodes d'analyse thermoéconomique appliquée à un système de cogénération,FRENCH THERMQUES CONGRESS "SFT, 2006, Ille de Ré, France, 126-131;
32. Lozano MA, and Valero, A. 1993, Theory of The exergetic cost, Energy 18(9), pp. 939-960
33. Mady CEK, Pinto CR, Pereira MTRM,*Application of the Second Law of Thermodynamics in Brazilian Residential Appliances towards a Rational Use of Energy*,Entropy, 2020, 22(6), 616,https://doi.org/10.3390/e22060616;
34. Montes MJ, Abanades A., Martinez-Val JM - Performance of a direct steam generation solar thermal power plant for electricity production as a function of the solar multiple, Solar Energy 83 (2009) 679–689
35. Montes MJ, Abanades A., Martinez-Val JM, Valdes M. - Solar multiple optimization for a solar-only thermal power plant, using oil as heat transfer fluid in the parabolic trough collectors, Solar Energy 83 (2009) 2165–2176
36. Moran, MJ, Shapiro, HN, Boettner, DD, Bailey, M.,B. Fundamentals of Engineering Thermodynamics. John Willey & Sons (2011)
37. Morin G., Dersch J., Platzer W., Eck M., Haberle A. - Comparison of Linear Fresnel and Parabolic Trough Collector power plants, Solar Energy 86 (2012) 1–12

38. Pop, OG, Magurean, AM, Pocola, AG, Ciocan, M., Zaaoumi, A., Balan, MC, 2021. Performances of Solar Thermal Collectors in Different Climatic Conditions, in: Moga, L., Șoimoșan, TM (Eds .), Environmental and Human Impact of Buildings. Springer Tracts in Civil Engineering. Springer, Cham.
39. Plank, M., The theory of heat radiation, Dover Publications, New York, 1959
40. Rohani S., Fluri TP, Dinter F., Nitz P, - Modeling and simulation of parabolic trough plants based on real operating data, Solar Energy 158 (2017) 845–860
41. Quaschning V., Understanding Renewable Energy Systems, Earthscan, London, 2007
42. Schenk H., Hirsch T., Feldhoff JF, Wittmann M. - Energetic Comparison of Linear Fresnel and Parabolic Trough Collector Systems, Journal of Solar Energy Engineering, 136 (2014) 041015-1
43. Serban A., Stefănescu MF, Năstase G., Ciocan M., Bucșa S., Dobrovicescu A., Exergetic Analysis of a Cogeneration System for Cooling and Heating,*UBT International Conference, 2018, Pristina, Kosovo*,https://knowledgecenter.ubt-uni.net/conference/2018/all-events/150, DOI 10.33107/ubt-ic.2018.150, ISBN978-9951-437-69-1
44. Shirazi, A., Taylor, RA, Morrison, GL, White, SD, 2018. Solar-powered absorption chillers: A comprehensive and critical review. Energy Convers. Manage. 171, 59-81.
45. StefanescuMF,PopE.,DobrovicescuA.,SerbianA.,HammerM.,JacobE., Chemical Analysis and Chemical Exergy of the Fuel Obtained from Municipal Waste,2018 IEEE International Conference on Environment and Electrical Engineering and 2018 IEEE Industrial and Commercial Power Systems Europe (EEEIC / I&CPS Europe), 12-15 June 2018, Palermo, Italy, DOI:10.1109/EEEIC.2018.8494425
46. Vekemans O., Chaouki J., Municipal Solid Waste Cofiring in Coal Power Plants: Combustion Performance,Developments in Combustion Technology, (2016) https://www.intechopen.com/chapters/51472
47. Zaaoumi, A., Bah, A., Ciocan, M., Sebastian, P., Balan, MC, Mechaqrane, A., Alaoui, M., 2021. Estimation of the energy production of a parabolic trough solar thermal power plant using analytical and artificial neural network models. Renewable Energy 170, 620-638.
48. Ziegler, B., Trepp, Ch., 1984. Equation of state for ammonia-water mixtures. International J. Refrig. 7, 101-106.
49. *** PTMx Parabolic Trough Collector – Technical data sheet, Soltigua 2014
50. https://www.ipcc.ch/sr15/
51. https://www.un.org/en/climatechange/net-zero-coalition
52. https://climate.ec.europa.eu/eu-action/european-green-deal/european-climate-law_en
53. https://commission.europa.eu/strategy-and-policy/priorities-2019-2024/european-green-deal_en
54. https://www.cnbc.com/2022/07/06/europe-natural-gas-nuclear-are-green-energy-in-some-circumstances-.html
55. https://www.oilandgasiq.com/events-methane-mitigation-europe/agenda-mc?utm_source=46366.001-Evolved_Google-PPC&utm_medium=CPC&utm_campaign=46034.001_Google_PPC_&utm_term=&utm_content=&disc=&extTreatId=7572173&gclid=CjwKCAiAwomeBhBWEiwAM43YIG068HpU3q5QkOCExD7kaLSAZ7WoWIlPKG7oV3e3vphQXm2dru8XPRoCijoQAvD_BwE
56. https://unfccc.int/process/transparency-and-reporting/greenhouse-gas-data/greenhouse-gas-data-unfccc/global-warming-potentials
57. https://www.myclimate.org/information/faq/faq-detail/what-are-negative-emissions/
58. http://en.wikipedia.org/wiki/Sun
59. http://en.wikipedia.org/wiki/Earth_physical_characteristics_tables
60. http://rredc.nrel.gov/solar/spectra/am1.5
61. http://hypertextbook.com/facts/1997/GlyniseFinney.shtml
62. https://re.jrc.ec.europa.eu/tmy.html
63. https://rredc.nrel.gov/solar/old_data/nsrdb/1991-2005/tmy3/by_state_and_city.html
64. https://www.nrel.gov/docs/fy08osti/43156.pdf

## Published articles

1. Ștefănescu MF, Pop E., Dobrovicescu A., Șerban A., Ciocan M., Iacob E., Chemical Analysis and Chemical Exergy of the Fuel Obtained from Municipal Waste, 2018 IEEE International Conference on Environment and Electrical Engineering and 2018 IEEE Industrial and Commercial Power Systems Europe (EEEIC/I&CPS EUROPE), Published: 2018, ISBN: 978-1-5386-5186-5, WOS: 000450163702042
2. Serban, A., Stefanescu, MF, Nastase, G., Ciocan, M., Bucsa, S., Dobrovicescu, A., Exergetic Analysis of a Cogeneration System for Cooling and Heating, 2018, UBT International Conference, PP 26-31 , DOI 10.33107/ubt-ic.2018.150, https://knowledgecenter.ubt-uni.net/cgi/viewcontent.cgi?article=1772&context=conference
3. Bucşă S., Năstase G., Şerban A., Ciocan M., Drughean L., Cooling and dehumidification systems used in air separation, 19 th International Multidisciplinary Scientific GeoConference Surveying Geology and Mining Ecology Management, SGEM 2019, Volume 19, Issue 6.1 , Pages 139 – 144, ISSN 13142704, ISBN 978-619740876-8, DOI 10.5593/sgem2019/6.1/S24.018
4. **Ciocan M**., Dobrovicescu A., Șerban A., Ștefănescu MF, Năstase G., Comparative energetic and exergetic analysis of individual or cogenerative systems with steam turbines for producing heat and mechanical work, 19 th International Multidisciplinary Scientific GeoConference Surveying Geology and Mining Ecology Management, SGEM 2019, Volume 19, Issue 6.1, Pages 109 – 116, ISSN 13142704, ISBN 978-619740876-8, DOI 10.5593/sgem2019/6.1/S24.014
5. Zaaoumi,A., Bah,A., Ciocan,M., Sebastian,P., Balan,MC, Mechaqrane,A., Alaoui,A. - Estimation of the energy production of a parabolic trough solar thermal power plant using analytical and artificial neural networks models, Renewable Energies, 170 (2021), pp. 620-638, ISSN: 0960-1481 (IF: 8.001 / 2020) https://doi.org/10.1016/j.renene.2021.01.129
6. Pop, OG, Dobrovicescu, A., Serban, A., Ciocan, M., Zaaoumi, A., Hiris, PD, Balan, MC - Analytical modeling of food storage cooling with solar ammonia-water absorption system, powered by parabolic trough collectors. Method, MethodsX 10C (2023) 102013, ISSN: 2215-0161 (JCI: 0.43 / 2021) https://doi.org/10.1016/j.mex.2023.102013